Solar Phys (2008) 249: 293–306
DOI 10.1007/s11207-008-9188-6

Observation of Turbulence in Solar Surface Convection: I. Line Parameter Correlations

A. Hanslmeier · A. Kučera · J. Rybák · H. Wöhl

Received: 22 December 2006 / Accepted: 8 April 2008 / Published online: 11 May 2008

Abstract By using slit observations of solar photospheric lines shifted by 0.4 arcsec, a 2D field on the Sun was scanned to obtain a 16-minute time series of 2D line-parameter variations. The aim was to investigate in detail the occurrence of turbulence that can be measured by line-width variations extracted from the line profiles. The continuum-intensity variation served as a proxy for granular (bright) and intergranular (dark) areas. The results show that turbulence is not limited to the intergranular space but is also produced by horizontal motions that may become supersonic, leading to turbulence. These motions lead to brightenings, as predicted by theoretical models. Thus, enhanced line-width variations are found to occur in both bright and dark areas. A Sobel filter served to detect the areas where strong gradients in the line parameters occur. By applying this filter to the different line-parameter variations over the 2D field observed, we can determine whether there exists a similarity of these strong-gradient patterns with other parameters that characterize granular motions such as intensity variations or velocity fluctuations.

Keywords Sun: granulation · Sun: photosphere · Turbulent convection

1. Introduction

The dynamics of solar granulation is a topic of great intrinsic interest and is important for the understanding of other phenomena such as acoustic flux generation or small-scale dynamos that are affected by it. Muller (1999) and more recently Stein *et al.* (2007) have reviewed the subject. High-spatial-resolution observations of solar granulation and several parameters

A. Hanslmeier (✉)
Institut für Physik, Geophysik Astrophysik Meteorologie, Univ.-Platz 5, 8010 Graz, Austria
e-mail: arnold.hanslmeier@uni-graz.at

A. Kučera · J. Rybák
Astronomical Institute, Slovak Academy of Sciences, 05960, Tatranská Lomnica, Slovakia

H. Wöhl
Kiepenheuer-Institut für Sonnenphysik, Schöneckstr. 6, 79104 Freiburg, Germany

that are relevant for theoretical modeling were discussed by Nesis *et al.* (2006). Among these parameters are the vertical gas velocity (v) and the line width (w). Nesis *et al.* found burst-like changes of these variables and mention a threshold at about 200 km altitude where the dynamics of the granulation should change. This threshold can be attributed to the decay of convectively driven motions there. The temperature–velocity correlation becomes zero, which means that convective motions no longer occur there.

We observed two photospheric lines: one with a core formation height just above that threshold and the other with a core formation height significantly above that value.

We give a short overview concerning acoustic wave excitation and turbulence. Upward propagating acoustic flux is assumed to be an important heating source for at least the lower chromosphere. The observation of the onset of acoustic flux requires high-spatial-resolution time series of photospheric lines. There are cases where acoustic-flux generation is related to the occurrence of turbulence; however, this is not valid in general.

1.1. Acoustic Flux and Oscillation Signatures

High-resolution observations of acoustic events and granulation were made by scanning 14 wavelength positions in the Fe I 543.4 nm line (Rimmele *et al.*, 1995). One scan took 32.5 seconds and time series of 108 and 65 minutes were recorded. Acoustic events were found: The local granulation becomes darker over several minutes and an abrupt darkening occurs immediately before the peak of the event. The stronger the acoustic event, the darker the granulation. Rimmele *et al.*'s conclusion is that rapid cooling in the upper convective layer leads to excitation of acoustic events. The acoustic events are always found near downflows.

It was proposed that solar acoustic oscillations are excited by localized cooling events observed as downflow plumes (Rast, 1999), and the excitation of chromospheric wave transients by collapsing granules was studied (Skartlien, Stein, and Nordlund, 2000). Granular motions are a result of mass conservation and a balance between upward transportation of internal energy and radiative cooling. As granules expand, the upflow velocity in the central parts is reduced, resulting in less internal energy flux. This process excites pressure waves. The surface radiative cooling dominates, the opacity is strongly reduced (because it varies as T^8 for continuous absorption from H^-), the gas becomes transparent, and the underlying gas cools radiatively. By this mechanism a downflowing thermal plume develops. Another scenario is the generation of sound by convectively driven turbulence (Bogdan, Cattaneo, and Malagoli, 1993).

In recent numerical simulations of acoustic wave propagation and dispersion in the non-magnetic solar subphotosphere and by making comparison with helioseismic observations, Shelyag, Erdélyi, and Thompson (2006) conclude that the source of acoustic flux is not located near the surface but below.

1.2. Shock Signatures

Shocks are regions where physical parameters change abruptly and play an important role for energy dissipation. Therefore, it is interesting to find the locations of these regions by observations. The expected changes in continuum intensity are small (Steffen, 1994) so white-light images do not give information about shocks and spectroscopic data are needed.

What are the signatures of shocks in the photosphere? From radiative transfer calculations several features are expected: significant increase of the line width, up to three times the normal value (Gadun and Hanslmeier, 2000) and up to two times when the data are corrected for degradation owing to the instrumental profile (Solanki *et al.*, 1996), an increase in the

residual intensity (as the shock heats the post-shock plasma; Gadun and Hanslmeier, 2000), and extreme jumps of line shifts (which if interpreted as Doppler shifts indicate strong velocity fluctuations there). The equivalent-width variations are small (since an increase in the line width is mainly compensated by an increase in the residual intensity). Other variations that concern line profiles have been discussed as well (Rybák *et al.*, 2004).

1.3. Turbulence Signatures

The increase in the line width reflects turbulent motions caused by the shocks. Therefore, we can expect that line-width observations serve as the most prominent proxy for shock occurrence. In our case the full width at half maximum of the line profiles was used as an indication of such processes. How do shocks and the generation of oscillations that lead to acoustic flux generation depend on each other?

Cattaneo, Hurlburt, and Toomre (1990) used numerical simulations with high spatial resolution to study the formation of regions of supersonic motions near the upper thermal boundary layer. Within these regions, the dynamics are dominated by nonstationary shock structures. These shocks form near the downflow sites and propagate upstream along the boundary layer to the upflow regions, where they weaken and disappear.

It was claimed that regions of supersonic horizontal flow form intermittently in the vicinity of the downflow lanes (Nesis *et al.*, 1992). The origin of solar oscillations, whether in the bright granular or dark intergranular elements, was investigated (Goode *et al.*, 1998). Seismic events, mainly observed in the intergranular lanes, may be the origin of p modes and not the deceleration of upgoing matter in the granules.

The different behavior of five-minute oscillations above granules and intergranular lanes was studied by using a 30-minute time series of the Fe I 5324 Å line profile (Khomenko, Kostik, and Shchukina, 2001). It was found that the most energetic intensity oscillations occur above intergranular lanes and the most energetic velocity oscillations occur above granules and lanes with the highest contrast. Indications of shock waves in the photosphere were studied also by Rybák *et al.* (2004). From these papers it follows that flux generation and shocks are connected.

Advanced numerical modeling techniques enabled Steffen (1994) to study acoustic flux generation in the solar convection zone. Another numerical experiment was made by Bogdan, Cattaneo, and Malagoli (1993). The total energy of the acoustic field is found to be a fraction of a percent of the kinetic energy of the convection.

In this paper we give some examples of line-parameter variations that are regarded as proxies for enhanced turbulence and shock formation and therefore also as a proxy for acoustic flux generation. We address the question of whether such processes are related to mostly granular or intergranular areas. By means of a Sobel filter, we can study sharp transitions of these line parameters that are indicative of shocks. Hanslmeier *et al.* (2006) presented initial results of this study.

2. Observations and Data Reduction

To seek out the occurrence of acoustic flux, we used a time series consisting of eight 2D scans performed with the Vacuum Tower Telescope (VTT) at the Observatorio del Teide. The data were taken on 22 June 1999 and a magnetically inactive region near the Sun's disk center was selected. The spatial sampling interval was 0.4 arcsec and the total scanned area was 12.8×20 arcsec. Since each exposure lasted for about 2.5 seconds, a total scan required 125 seconds.

Two lines were studied: *i*) a higher Fe I line, λ 630.1508 nm, with an equivalent width of 127 mÅ and formation of its line core at a height of 378 km, and *ii*) a deeper Fe I line, λ 630.2499 nm, with an equivalent width of 83 mÅ and a height of line core formation at 270 km. The observations yield the line profiles, and from these continuum intensity (I_c), line center intensity (r_c), full width at half maximum (w), and line center position related to the line center velocity (v_c) were obtained.

A detailed description of the observations and data reduction has been given by Hanslmeier *et al.* (2004).

In this paper we used a Sobel filter to detect and enhance the regions where strong gradients of line parameters occur. The filter is obtained as follows. Let F_{jk} denote the pixels in an image F. Then the Sobel filter G_{jk} is defined by

$$G_{jk} = |G_x| + |G_y|, \tag{1}$$

where G_x and G_y are given by

$$G_x = F_{j+1,k+1} + 2F_{j+1,k} + F_{j+1,k-1} - (F_{j-1,k+1} + 2F_{j-1,k} + F_{j-1,k-1}), \tag{2}$$

$$G_y = F_{j-1,k-1} + 2F_{j,k-1} + F_{j+1,k-1} - (F_{j-1,k+1} + 2F_{j,k+1} + F_{j+1,k+1}). \tag{3}$$

As can be seen easily from numerical experiments, a 2D array that varies homogeneously without sharp transitions does not show any contours after applying a Sobel filter. When parameters vary sharply, the Sobel filter significantly enhances those features. From the discussion in the literature it is evident that we should expect the occurrence of turbulence at these sharp gradients (*e.g.*, leading to a significant increase in line width).

3. Results

First we give histograms showing the distributions of the line parameters and the temporal evolution of these histograms. In Figure 1 the histograms of the line parameters for the deeper line are given as they have been calculated from the line profiles. The different curves show the histograms for different time steps. In the histograms for each time step, 200×102 data points have been used. All panels in Figure 1 clearly show that the distributions are slightly asymmetric. To check the behavior over granular and intergranular areas, we applied a separation according to the continuum intensity (I_c):

- Dark intergranular areas were defined as regions where $I_c < 0.92$.
- Bright granular areas were defined where $I_c > 1.08$.

Then the behavior of the full width at half maximum (w, given in mÅ) was investigated according to these values. In Figure 2 it is clearly demonstrated that for $I_c < 0.92$ there is a scatter of w around 120 mÅ; for $I_c > 1.08$ the values of w are lower on average (by about 10%) but some may also occur near the values found for intergranular areas. This is also clearly seen in the histograms given by Figure 3. We see that low w values (dotted) predominantly occur in the granular areas, as well as negative (blueshifted) v_c values. For r_c, there is no clear tendency.

It was found that the histograms for the higher line are similar and therefore they are not given here. Enhanced turbulence manifests itself in a line broadening (Nesis *et al.*, 1992) in the vicinity of downflow lanes. Turbulence, and in some cases acoustic flux, is expected to occur near sharp transitions of line parameters (see, *e.g.*, Nesis *et al.*, 1992; Goode *et al.*,

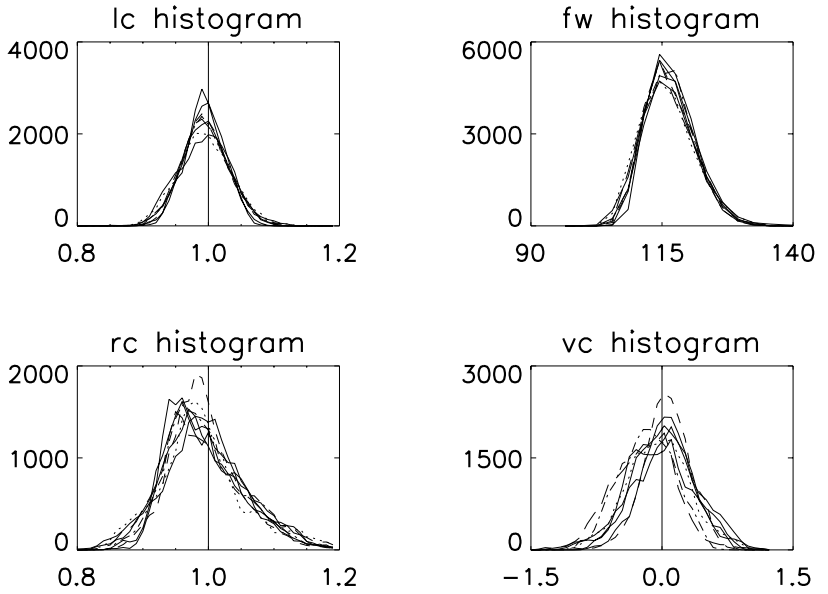

Figure 1 Histograms of the line parameters I_c, w, v_c, and r_c derived from the deeper originating line. I_c and r_c are normalized and w and v_c are given in the physical units of mÅ and km s^{-1}, respectively.

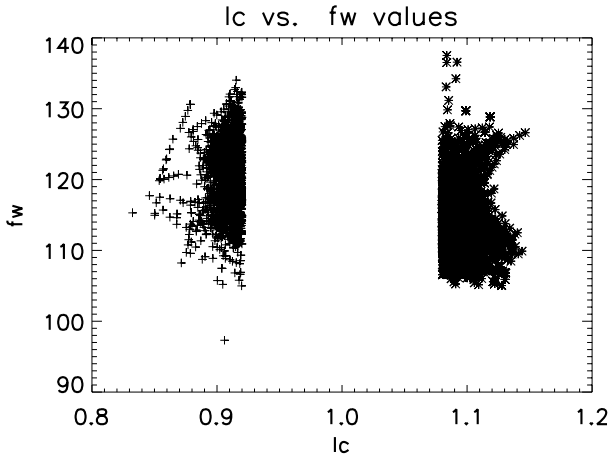

Figure 2 Line parameter w plotted as a function of low I_c (+) and high I_c (*). The higher-laying line was used.

1998) the Sobel filter seems to be adequate to enhance these regions of sharp transitions of the line parameters.

In Figures 4 and 5 the original line parameters are plotted and the Sobel-filtered data are plotted over the image of the line parameter variations (with the spatial size corresponding to 12.8 ×20 arcsec). The Sobel data were reduced by a factor of three to enable us to discern the original data in the images.

Therefore these figures indicate regions of great variation of the line parameters. In Figure 4, the line parameters for the higher line are shown as a function of time. The image at the bottom is the first in the time series. From left to right the columns are I_c, w, v_c,

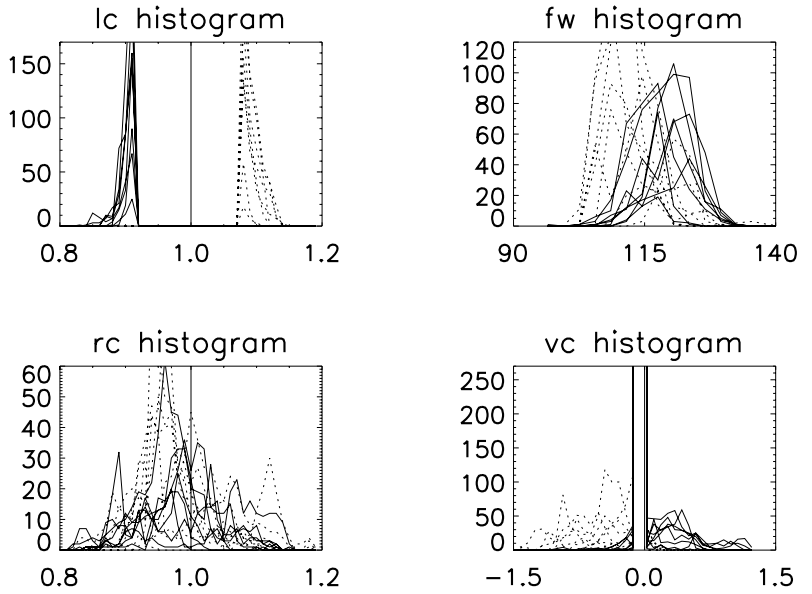

Figure 3 Histograms showing the distributions of the line parameters for high (dotted) and low I_c (solid). The deeper laying line was used.

and r_c. The edges are strongly enhanced and more pronounced by the Sobel filter than in the original images (which are not given here). In Figure 5, the same is shown for the deeper line.

Both figures enable us to follow the evolution of the structures of the line parameters over a time span of roughly 16 minutes. Comparing the two figures we also see that the structures for the higher and deeper line are quite similar, with the greatest difference being found for the w parameter.

To quantify the relations with and without Sobel filtering, the behavior of the correlations between the different line parameters was studied. The correlations were calculated over each of the eight images from 2D scans in the time series. Thus eight values were obtained. In this paper we only consider correlations that may be important for acoustic flux.

Figure 6 gives the results for the deeper originating line and Figure 7 for the higher originating line. Since the field investigated has only a small area (12.8×20 arcsec) the evolution of the granulation influences the data as well as the five-minute oscillations, which were not eliminated. Both effects contribute to the temporal variation of the data.

For the unfiltered data, the correlation $\langle I_c, w \rangle$ (full line) varies between -0.4 and -0.2. This means that enhanced w values are weakly correlated with smaller I_c values. The enhanced w fields correspond to mainly darker intergranular fields. Applying the Sobel filter changes the results completely: The correlation values become very small and the sign is changed. This means that there seems to be a very weak correlation between enhanced w and enhanced I_c values. The results are very similar for both lines.

For the deeper line, the correlation $\langle r_c, w \rangle$ (long dashed) is positive and fluctuates between 0.5 and 0.6. Applying the Sobel filter reduces it to 0.35. For the higher line the values are lower (0.5 down to 0.3) and the strong fluctuations are again reduced by applying the Sobel filter and become constant around 0.3 similar to that of the deeper line.

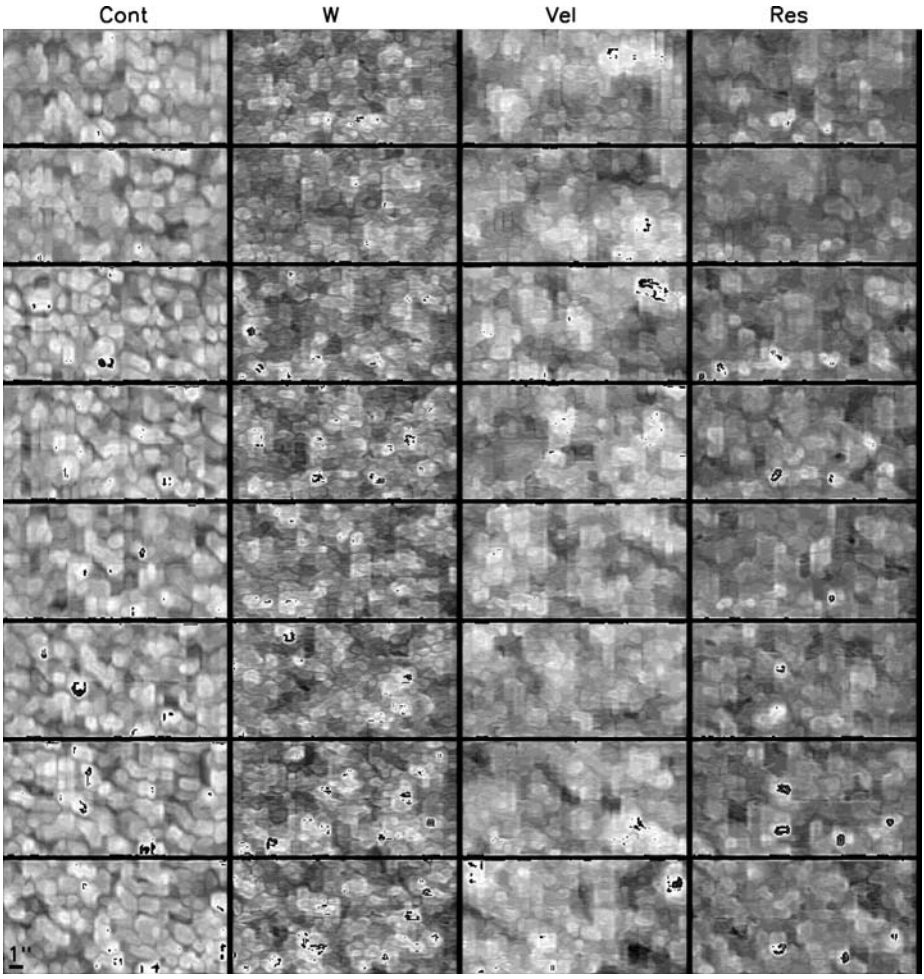

Figure 4 Higher line: Evolution of line parameters. The Sobel-filtered data are overlaid so that the edges are strongly enhanced. Columns 1, 2, 3, and 4 denote $I_c(0.27)$, $w(16)$, $v_c(20)$, and $r_c(60)$, respectively. The difference of the variation from minimum to maximum values is given in parentheses. The scale is indicated in the lower-left panel.

For the deeper originating line, the correlation $\langle I_c, v_c \rangle$ (dotted line) varies between -0.4 and -0.6. For the higher line, the correlation is lower (-0.2 to -0.3) because of the influence of oscillations that grow with height in the photosphere. After the Sobel filter is applied, the correlation changes sign and becomes stable near 0.3 in the case for the deeper line and near the value of 0.2 for the higher line.

For the deeper originating line, the correlation $\langle I_c, r_c \rangle$ (dashed line) is zero and slightly enhanced to 0.2 after application of the Sobel filter. For the higher line, it is also very low for the unfiltered data and enhanced to 0.2 for the Sobel-filtered data.

For the deeper forming line, the correlation $\langle v_c, w \rangle$ (dashed-dotted line) is positive for both filtered and unfiltered data, showing pronounced variations along the time series that may be attributed to oscillations. The values are about 0.2 and the positive sign indicates that

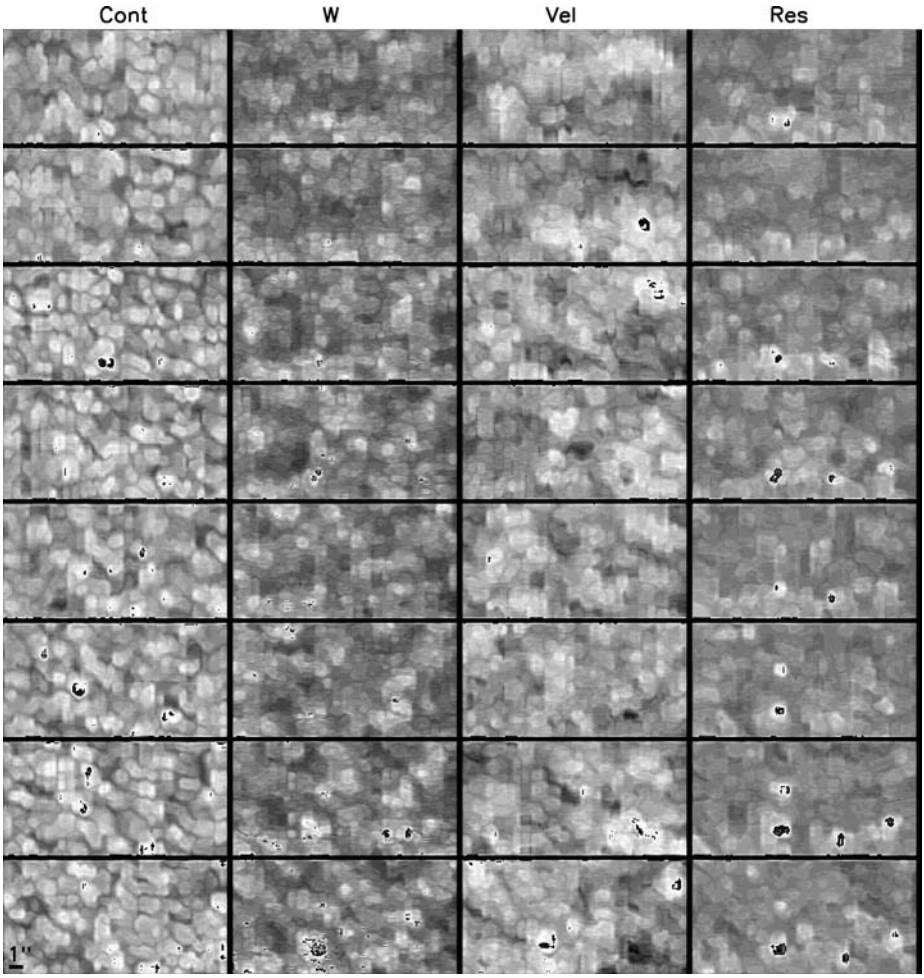

Figure 5 Deeper line: Evolution of line parameters. The Sobel-filtered data are overlaid so that the edges are strongly enhanced. The difference of the variation from minimum to maximum values introduced by the Sobel filter is given in parentheses. Columns 1, 2, 3, and 4 denote $I_c(0.27)$, $w(17)$, $v_c(19)$ and $r_c(92)$, respectively. The scale is indicated in the lower-left panel.

enhanced w values correspond to downflows (positive sign of velocity fluctuations). Similar statements can be given for the higher line. The Sobel filter strongly reduces the fluctuations.

The correlation $\langle v_c, r_c \rangle$ (dashed-dotted-dotted-dotted) exhibits similar behavior for both lines, with fluctuations reduced after Sobel filtering.

Figures 8 and 9 give three columns of images. In the first column there are eight images of continuum intensity. The time evolution is shown from bottom to top. The data shown in the next two columns have been selected by the following criteria: *i*) enhanced I_c (bright granulum) and enhanced w (white); *ii*) reduced I_c (dark intergranulum) and enhanced w (gray); and *iii*) regions where the vertical velocities are very small (denoted in gray in the outermost right column in the figures). The enhanced w was defined as

$$\text{average}(w) + \big[\max(w) - \min(w)\big]/10,$$

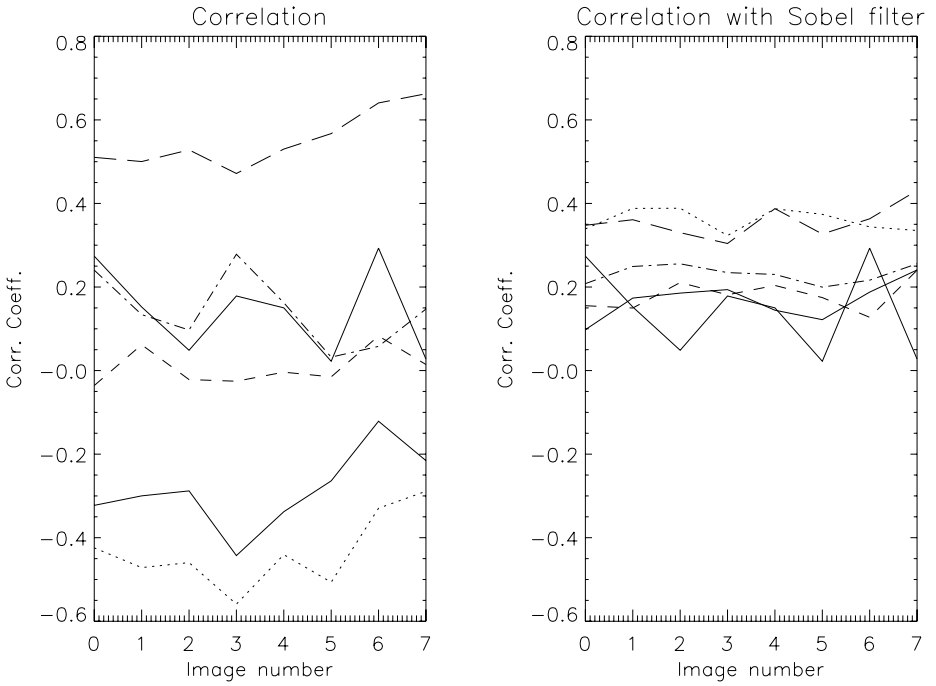

Figure 6 Deeper line: Evolution of correlation coefficients for (left) the original line parameters and (right) the filtered parameters: $\langle I_c, w\rangle$ (full line), $\langle r_c, w\rangle$ (long dashed line), $\langle I_c, v_c\rangle$ (dotted line), $\langle I_c, r_c\rangle$ (dashed line), $\langle v_c, w\rangle$ (dashed-dotted line), and $\langle v_c, r_c\rangle$ (triple-dotted-dashed line).

the enhanced continuum was defined as

$$\text{average}(I_c) + \big[\max(I_c) - \min(I_c)\big]/30,$$

and the small vertical velocities were defined by

$$v_m = \big[\max(v) - \min(v)\big]/60, \quad -v_m < v < v_m.$$

Figure 8 shows the results for the higher forming line and Figure 9 shows those for the deeper forming line.

The regions of low vertical velocities show a rapidly evolving larger scale pattern. There is no resemblance with granular-like structures. Regions of reduced I_c and enhanced w are larger than regions with enhanced I_c and enhanced w. In both cases the figures of the higher and deeper lines are similar. It is seen that there occur areas where both I_c and w are high and areas where I_c is low and w is high.

Summarizing, we can state that the continuum evolution and other line-parameter evolution can be clearly followed in the time series. Enhanced w regions occur both in bright granular areas as well as in dark intergranular areas. The Sobel filter enables us to detect edges and to enhance them. The Sobel-filtered w values show a stochastic pattern that does not seem to be related to the granular field. The fields evolve rapidly and corresponding patterns are hardly recognized after two minutes.

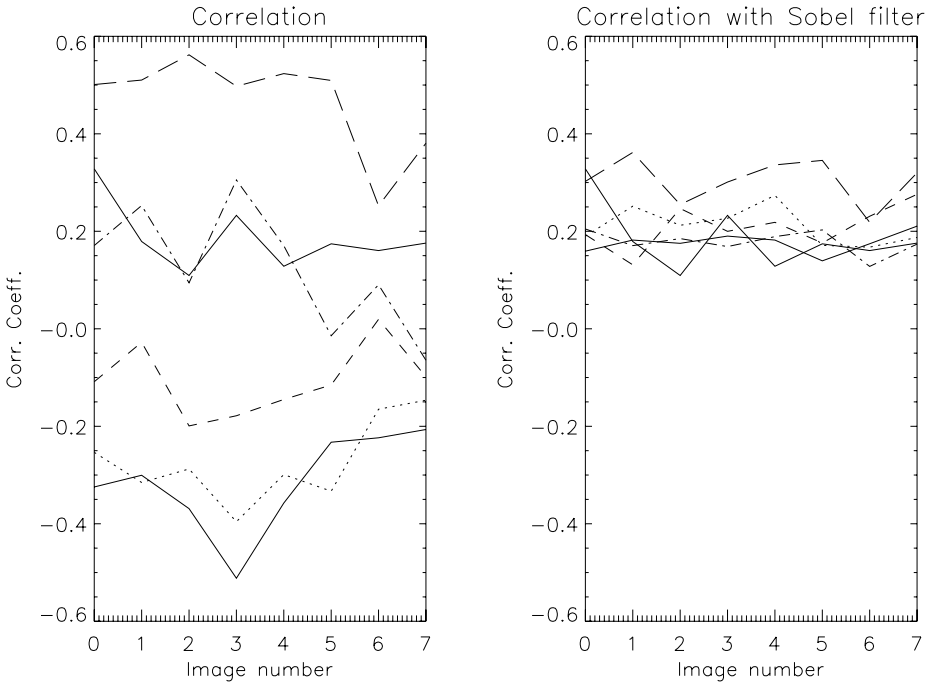

Figure 7 Higher line: Evolution of correlation coefficients for (left) the original line parameters and (right) the filtered parameters. See description of lines in previous figure.

4. Discussion

First we have to mention that the data were not filtered for the five-minute oscillations because a true filtering in the $k-\omega$ domain was not possible. The evolution of the correlations from image one to eight may be related to the five-minute oscillation but also to the evolution of the granular/intergranular field. Oscillations increase in amplitude with height. Therefore the correlation $\langle I_c, v_c \rangle$ (dotted lines in Figures 6 and 7) for both lines is different: The values are larger for the deeper line than for the higher line. This can be explained by the fact that for the deeper line convective motions dominate. Thus upward motion is mainly correlated with bright granules and downward motion with darker intergranular areas. After the application of a Sobel filter this correlation changes sign, becoming slightly positive for the deeper as well as for the higher line. This can be interpreted in the sense that there is a tendency for regions of strong velocity gradients to correspond to regions with strong gradients of the continuum intensity (temperature field).

Let us consider in particular the correlation $\langle I_c, w \rangle$. As predicted by different authors (*e.g.*, Hoekzema, Rimmele, and Rutten, 2002), enhanced turbulence and rapid variations of continuum intensity owing to rapid granular decay should also indicate acoustic flux. In our original data, enhanced I_c is correlated with lower w values, indicating that turbulence predominantly occurs in darker intergranular areas. The fact that after application of the Sobel filter the sign of the correlation changes can be interpreted as follows: Regions of strong w variations correspond weakly to regions of strong I_c variations.

Results from radiative-transport calculations that were mentioned in the introduction already show that residual intensity variations may be more appropriate to reflect shock sig-

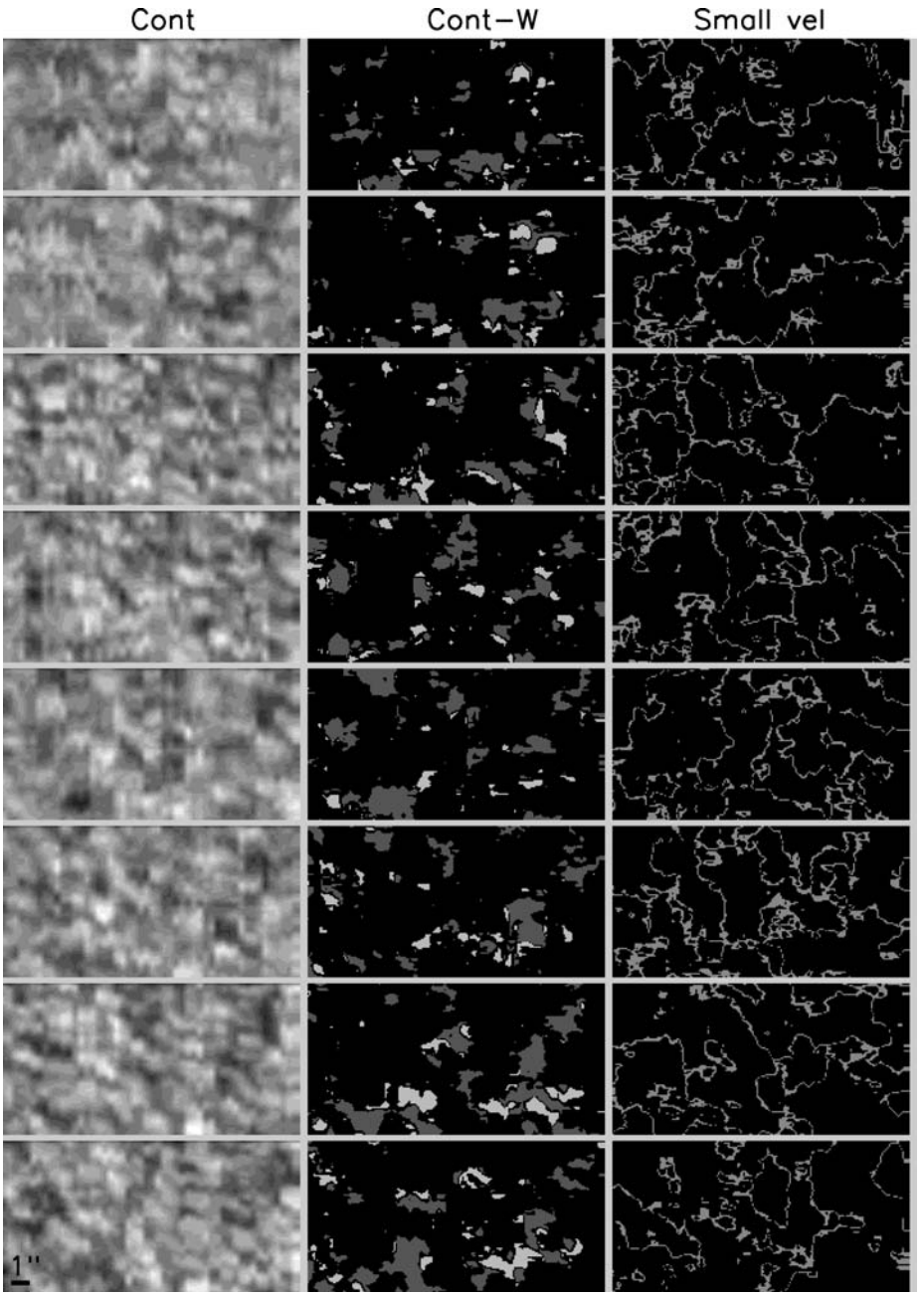

Figure 8 Higher line: Evolution of (left) continuum intensity, (middle) regions of enhanced I_c and w (white) and regions of reduced I_c and enhanced w (gray), and (right) regions with only small vertical velocity. The scale is indicated in the lower-left panel.

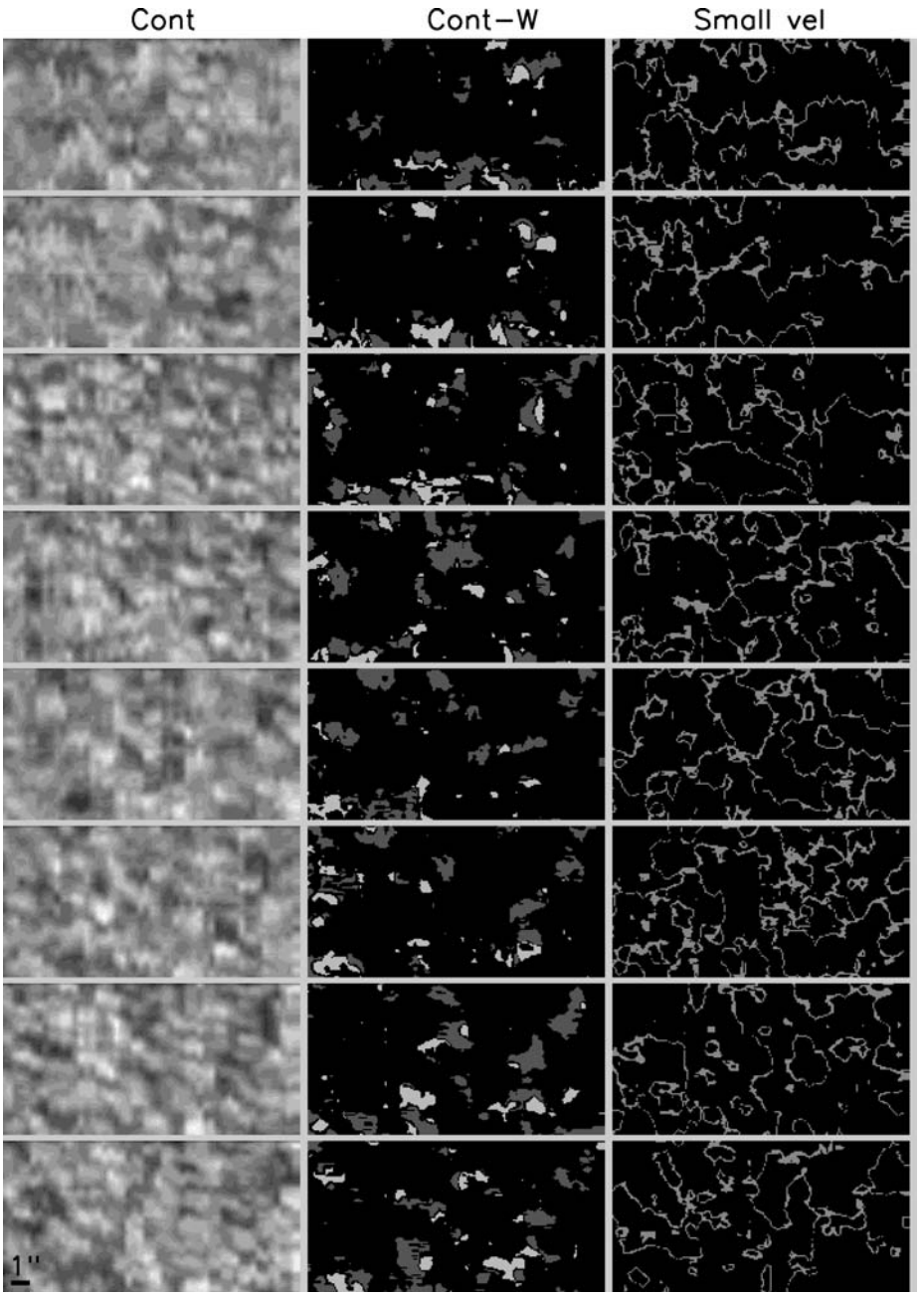

Figure 9 Lower line: Evolution of (left) continuum intensity, (middle) regions of enhanced I_c and w (white) and regions of reduced I_c and enhanced w (gray), and (right) regions with only small vertical velocity. The spatial scale is indicated in the lower-left panel.

natures. We find a stronger correlation ($\langle r_c, w\rangle$) for the deeper line in the case of original data (compare Figures 6 and 7). The correlation is positive, which means that enhanced r_c values correspond to enhanced w values. For the higher line, the correlation is weaker and the fluctuation along the time is stronger, which indicates the influence of oscillations. The Sobel-filtered data show quite similar results for both lines. Regions of strong r_c gradients correspond weakly (with correlation in both cases near 0.3) to regions of enhanced w gradients. As to be expected from theory, this effect is more pronounced for the $\langle r_c, w\rangle$ data than for the $\langle I_c, w\rangle$ data (full line).

The values of the correlations are low but the temporal evolution suggests some consistency and thus the results at least are a strong hint for horizontal shocks that are connected with turbulence and enhanced brightenings. Rast (1999) and Skartlien and Rast (2000) studied a compressible thermal starting plume as an acoustic source. Their conclusion was that the source of the excitation mechanisms must be either a negative pressure fluctuation associated with photospheric darkening or a positive pressure fluctuation with a brightening. Skartlien, Stein, and Nordlund (2000), in their study of acoustic waves in the chromosphere that are excited by the collapse of small granules, found that the upflow reverses to a downflow on a time scale shorter than three minutes (acoustic cutoff period).

Comparing Figures 6 and 7 one sees that, for the Sobel-filtered data, the fluctuations and correlations for the deeper line are significantly larger than for the higher laying line. This may also hint at the greater influence of granular/intergranular evolution in the deeper photosphere.

We also investigated the correlation of I_c with the Sobel w data and the correlation of the v_c with the Sobel w data for both lines. Both correlations were found to be near zero for both lines. The correlations of r_c with Sobel w were found to be around 0.3 for the deeper line and near 0.1 for the higher laying line. This demonstrates that for the deeper line convective turbulence becomes more important, with regions of strong w gradients weakly correlating with enhanced r_c values, which means enhanced temperature at the line core formation height level. We must take into account that the line-core formation height of the deeper line is still quite high.

The stochastic nature of the occurrence of turbulence is demonstrated by the chaotic pattern that is obtained after applying a Sobel filter to the w data (see second column of Figures 4 and 5). The images obtained are only weakly correlated with the granular field, as is also shown by the low, but positive, correlation between $\langle I_c, w\rangle$. Moreover, the structures in w differ greatly between different time steps.

The areas where both I_c and w are enhanced are often found near the areas where I_c is reduced and w is enhanced (see Figures 8 and 9). This can be interpreted as the fact that enhanced w values are correlated both with enhanced and reduced continuum intensity values. Interpreting enhanced w values as signatures of turbulence, the aforementioned observational fact could mean that *i*) w enhanced in intergranular areas are signatures of enhanced turbulence in the darker intergranular lanes and *ii*) enhanced w in enhanced I_c values are signatures of brightenings resulting from horizontal shocks. Comparing the third column of Figures 8 and 9 with the middle columns we see a slightly better correspondence of the small contour-like features of small vertical velocities with enhanced w values.

The histograms of the data show an asymmetry of the parameters and that the line parameter continuum intensity is insufficient to define clearly granular/intergranular structures. Brighter structures could also be caused by shocks and a signature for that is the distribution of r_c values evenly distributed over bright and dark structure (I_c) values. An enhancement of r_c could arise from shocks.

It is interesting to compare these results with those of Khomenko, Kostik, and Shchukina (2001). In that paper the occurrence of five-minute oscillations in granular/intergranular

areas is discussed. They found that most energetic intensity oscillations occur above intergranular lanes whereas the most energetic velocity oscillations occur above granules and lanes with the maximum contrast. The Sobel filter used in our paper shows regions of high contrast.

The decay of convective cells resulting in intergranular areas and resembling in the scenario given by Rast (1999) and Skartlien and Rast (2000) may be associated with the regions of enhanced w and small I_c. There seems to be no significant difference between the two lines. However, to observe the relation with convective motions in more detail, spectral scans of deeper forming spectral lines would be needed.

Acknowledgements The authors thank the referees for their constructive comments. A.H. thanks the "FWF" for supporting these investigations. A.K. and J.R. acknowledge the grant VEGA 2/6195/26 and the German DFG Grant No. 436 SLK 113/7 and A.H., A.K., and J.R. acknowledge the Austrian and Slovak Academy of Sciences. The Vacuum Tower Telescope is operated by the Kiepenheuer Institut für Sonnenphysik, Freiburg, at the Observatorio del Teide of the Instituto de Astrofísica de Canarias.

References

Bogdan, T.J., Cattaneo, F., Malagoli, A.: 1993, *Astrophys. J.* **407**, 316.
Cattaneo, F., Hurlburt, N.E., Toomre, J.: 1990, *Astrophys. J.* **349**, L63.
Gadun, A., Hanslmeier, A.: 2000, *Kinemat. Fiz. Nebes. Tel* **16**, 130.
Goode, P.R., Strous, L.H., Rimmele, T.R., Stebbins, R.T.: 1998, *Astrophys. J.* **495**, L27.
Hanslmeier, A., Kučera, A., Rybák, J., Wöhl, H.: 2004, *Solar Phys.* **223**, 13.
Hanslmeier, A., Kučera, A., Rybák, J., Wöhl, H.: 2006, *Cent. Eur. Astrophys. Bull. CEAB* **30**, 11.
Hoekzema, N.M., Rimmele, T.R., Rutten, R.J.: 2002, *Astron. Astrophys.* **390**, 681.
Khomenko, E.V., Kostik, R.I., Shchukina, N.G.: 2001, *Astron. Astrophys.* **369**, 660.
Muller, R.: 1999, In: Hanslmeier, A., Messerotti, M. (eds.) *Motions in the Solar Atmosphere*, *ASSL* **239**, Kluwer, Dordrecht, 35.
Nesis, A., Bogdan, T.J., Cattaneo, F., Hanslmeier, A., Knoelker, M., Malagoli, A.: 1992, *Astrophys. J.* **399**, L99.
Nesis, A., Hammer, R., Roth, M., Schleicher, H.: 2006, *Astron. Astrophys.* **451**, 1081.
Rast, M.P.: 1999, *Astrophys. J.* **524**, 462.
Rimmele, T.R., Goode, P.R., Harold, E., Stebbins, R.: 1995, *Astrophys. J.* **444**, L119.
Rybák, J., Wöhl, H., Kučera, A., Hanslmeier, A., Steiner, O.: 2004, *Astron. Astrophys.* **420**, 1141.
Shelyag, S., Erdélyi, R., Thompson, M.J.: 2006, *Astrophys. J.* **651**, 576.
Skartlien, R., Rast, M.P.: 2000, *Astrophys. J.* **535**, 564.
Skartlien, R., Stein, R.F., Nordlund, A.: 2000, *Astrophys. J.* **541**, 468.
Solanki, S.K., Ruedi, I., Bianda, M., Steffen, M.: 1996, *Astron. Astrophys.* **308**, 623.
Steffen, M.: 1994, In: Schüssler, M., Schmidt, W. (eds.) *Solar Magnetic Fields*, Cambridge Univ. Press, Cambridge, 294.
Stein, R.F., Benson, D., Nordlund, A., Schaffenberger, W.: 2007, In: Stancliffe, R.J., Dewi, J., Houdek, G., Martin, R.G., Tout, C.A. (eds.) *Unsolved Problems in Stellar Physics*, *A.I.P. Conf. Ser.* **948**, Am. Inst Phys., Melville, 111.